Measurement of acoustic dissipation occurring in narrow channels with wet wall

Yuki Ueda[a] and Naoyuki Ogura
Department of Bio-Functions and Systems Science, Tokyo University of Agriculture and Technology, Nakacho 2-24-16, Koganei, Tokyo 184-8588, Japan

(Received 2 July 2018; revised 22 November 2018; accepted 7 December 2018; published online 4 January 2019)

The acoustic dissipation that occurs in a porous medium is experimentally investigated. Two conditions are tested. One is that the wall of the porous medium is wet by water, and the other is that it is dry. Experimental results show that water does not affect viscous dissipation; however, it affects the dissipation caused by pressure oscillation. Furthermore, it is found that the effect of water on the dissipation due to pressure oscillation increases with the temperature of the working gas. A theory that can consider the effect of condensation and evaporation on sound propagation is used to investigate the result. The theoretically and experimentally obtained values of dissipation are in good agreement. The reason for the effect of water is analyzed using the theory.
 https://doi.org/10.1121/1.5085775

[OU] Pages: 71–76

I. INTRODUCTION

Acoustic wave propagation in a gas-filled tube is a classical problem in fluid dynamics. Several researchers, such as Helmholtz, Kirchhoff, and Rayleigh, have derived theories to describe this phenomenon. (See the literatures listed in Ref. 1.) Tijdeman used the limit conditions that are suitable for treating engineering acoustics and obtained a simple expression for acoustic propagation.[1] Yazaki *et al*. measured the propagation constant in a cylindrical tube, and their results were in good agreement with theoretical values.[2]

A few experimental studies show the effect of the condensation and evaporation of a working gas on acoustic propagation. For example, Pandit and King measured the sound speed in sandstone and showed that the sound speed decreases by 20%–30% when relative humidity (RH) is increased to 98%.[3] Experimental results have motivated researchers to derivate advanced acoustic theories.[4–8] In these theories, an acoustic wave propagating in a cylindrical tube is considered. However, complex channels, such as the interior of sandstone,[3] are used in experiments. This implies that there are extremely few experimental results that can be qualitatively compared with theoretical results.

In this study, we have measured acoustic power dissipation in a porous medium with uniform narrow channels. The measurements are performed under two conditions. One is that the wall of the porous medium is wet, and the other is that it is dry. The obtained data indicate that the acoustic dissipation due to velocity oscillation under the wet condition is comparable to that under the dry condition. On the contrary, the acoustic dissipation due to pressure oscillation under the wet condition is larger than that under the dry condition. Experimental results are compared with the numerical results obtained based on the theory proposed by Raspet *et al*.,[5–7] and good agreement is obtained between the results.

The rest of this paper is organized as follows: Secs. II and III describe the experimental setup and measurement method, respectively. Section IV presents experimental results, and Sec. V shows their comparison with theoretical results. The results are summarized in Sec. VI.

II. EXPERIMENTAL SETUP

Figure 1 shows the schematic illustration of the constructed experimental setup. It essentially comprises three components, i.e., an acoustic driver (speaker), a water bath, and a resonator. The acoustic driver (Fostex model FW160N, Foster Electric Company, Tokyo, Japan) is electronically connected to a signal generator (Tektronix model AFG1062, Tektronix, Beaverton, Oregon) via an audio amplifier (Yamaha model P2500S Yamaha Corporation, Hamamatsu, Japan), and it inputs an acoustic wave to the resonator. The internal diameter of the resonator is 40 mm, and its length is approximately 2.2 m. The resonator is covered by the water bath to eliminate thermoacoustic effects[9–12] and to control the temperature (T_{gas}) of the gas inside the resonator; T_{gas} is controlled between 30 °C and 75 °C by changing the temperature of the hot water flowing in the water bath. The temperature (T_{gas}) is measured using thermocouples installed in the resonator, which are not shown in Fig. 1. The frequency of the input acoustic wave is set as 145 Hz, which is approximately the frequency of the second mode in the resonator. This implies that the amplitude of oscillatory pressure becomes the maximum close to the center of the resonator, whereas the amplitude of oscillatory velocity becomes the minimum close to the center.

The space in the resonator is divided into two parts (section 1 and section 2) by an elastic membrane. This realizes the following two conditions: The first is that the acoustic wave travels through the entire space in the resonator. This is because the acoustic wave passes through the membrane. The second is that the working fluids in the two sections do not mix. The working gas in section 1 is room air whose

[a]Electronic mail: uedayuki@cc.tuat.ac.jp

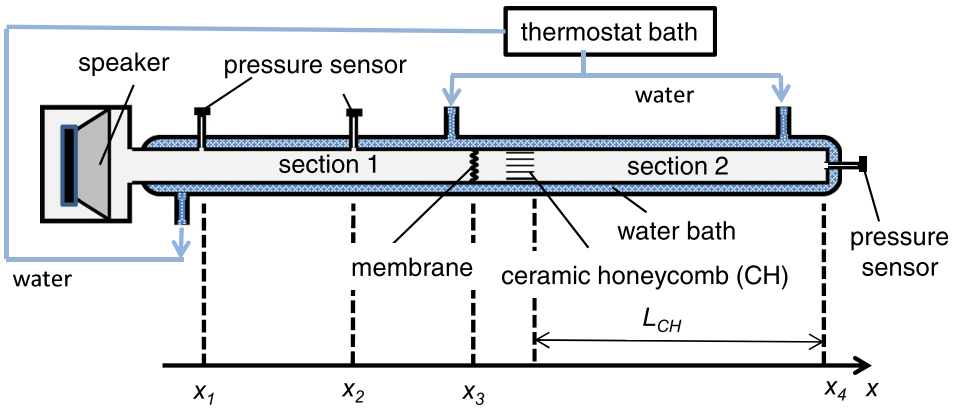

FIG. 1. (Color online) Schematic illustration of the experimental setup.

absolute humidity is lower than 12 g/m^3. The effect of the membrane on the measurements is discussed in Sec. III A.

A ceramic honeycomb (CH) is inserted in section 2 (see Fig. 1), and the distance between the closed end of the resonator and the CH, L_{CH}, is 0.59 m or 1.13 m. The reasons for this are straightforward. First, a CH can easily contain water on its wall. Second, it consists of numerous narrow channels, and hence, the acoustically dissipated power inside it is larger than that outside it. As a result of this, the effect of water can be investigated. Finally, the use of a CH enables us to classify dissipation into two types, i.e., the acoustic power dissipation caused by pressure oscillation and that caused by velocity oscillation. The pressure-oscillation-based dissipation becomes dominant when a CH is located at the position ($L_{\mathrm{CH}} = 1.13$ m) close to a pressure antinode, whereas the velocity-oscillation-based dissipation becomes dominant when it is located at the position ($L_{\mathrm{CH}} = 0.59$ m) close to a velocity antinode.

The cross section of the channels of the used CH is square. Half the length of one side of the square cross section is 0.47 mm. The CH is dipped into water to wet the surface of its wall. The water contained in the CH is controlled to be 5.0 ± 0.1 g.

A humidity meter (Toplas Engineering model TA50 Toplas Engineering Corporation, Tokyo, Japan) is temporally installed into section 2, and the humidity is checked with changing T_{gas}. It is found that the RH in section 2 increases owing to the water contained in the CH and depends on the position. The RH measured close to the CH and close to the closed end was 90%–100% and approximately 80%, respectively, when T_{gas} is higher than 50 °C. Note that the mean pressure inside the resonator is maintained at atmospheric pressure, independent of T_{gas}.

To measure oscillatory pressure, three pressure sensors (Jtekt model PD104, Jtekt Corporation, Nagoya, Japan) are set on the wall of the setup (see Fig. 1) via a small diameter tube whose internal diameter is 1 mm and length is 25 mm. The effect of this tube on pressure measurements is examined,[13] and the correction for this effect is performed.

III. METHOD OF EVALUATING ACOUSTIC DISSIPATION

As shown in Fig. 1, acoustic pressure oscillation is measured at two points on the wall of section 1. The theory used to evaluate the power dissipated in section 2, W_2, using the two measured values of pressure is described below.

A few expressions are used to describe acoustic wave propagation in a tube. Rott's formula, which is frequently used for analyzing thermoacoustic devices, is used in this study.[14] When the x axis is defined along a tube, the momentum and continuity equations[14,15] of Rott's formula can be written as

$$\frac{dP}{dx} = -\frac{i\omega\rho_m}{1-\chi_v}U, \tag{1}$$

$$\frac{dU}{dx} = -\frac{i\omega[1+(\gamma-1)\chi_\alpha]}{\gamma P_m}P. \tag{2}$$

Here, P and U are the acoustic-oscillatory pressure and velocity, respectively; ω is angular frequency; ρ_m, P_m, γ, and σ are the mean density, mean pressure, ratio of specific heats, and Prandtl number of the working gas, respectively; χ_α and χ_ν are complex functions,[14–16] which are mentioned below. Note that U is the cross-sectional mean value and P and U are complex values. For the case of a circular-cross section tube, the functions, χ_α and χ_ν, depend on

$$Y_\alpha = (i-1)\sqrt{\omega\tau_\alpha}, \tag{3a}$$

$$Y_\nu = (i-1)\sqrt{\omega\tau_\nu}, \tag{3b}$$

and they can be expressed as[14–16]

$$\chi_\alpha = \frac{2J_1(Y_\alpha)}{Y_\alpha J_0(Y_\alpha)}, \tag{4a}$$

$$\chi_\nu = \frac{2J_1(Y_\nu)}{Y_\nu J_0(Y_\nu)}, \tag{4b}$$

where τ_α and τ_ν are the thermal relaxation time and viscous relaxation time, respectively.[16] They are defined as

$$\tau_\alpha = r^2/(2\alpha), \tag{5a}$$

$$\tau_\nu = r^2/(2\nu), \tag{5b}$$

where r is the tube radius, α is the thermal diffusivity of the working gas, and ν is its kinematic viscosity.

Equations (1) and (2) can be solved analytically. Using the solution, the pressure and cross-sectional mean velocity at $x = x_b$ can be expressed in terms of those at $x = x_a$ as[17]

$$\begin{pmatrix} P(x_b) \\ U(x_b) \end{pmatrix} = M(x_a, x_b) \begin{pmatrix} P(x_a) \\ U(x_a) \end{pmatrix}$$
$$M(x_a, x_b) \equiv \begin{pmatrix} m_{11}(x_a, x_b) & m_{12}(x_a, x_b) \\ m_{21}(x_a, x_b) & m_{22}(x_a, x_b) \end{pmatrix}$$
$$m_{11}(x_a, x_b) = \cos\big(k(x_b - x_a)\big)$$
$$m_{12}(x_a, x_b) = -iZ_0 \sin\big(k(x_b - x_a)\big)$$
$$m_{21}(x_a, x_b) = \frac{-i}{Z_0} \sin\big(k(x_b - x_a)\big)$$
$$m_{22}(x_a, x_b) = \cos\big(k(x_b - x_a)\big). \tag{6}$$

Here, k and Z_0 are the complex wave number and characteristic impedance, respectively, and they are calculated as

$$k = \frac{\omega}{c} \sqrt{\frac{1 + (\gamma - 1)\chi_\alpha}{1 - \chi_\nu}} \tag{7}$$

and

$$Z_0 = \rho_m \frac{\omega}{k(1 - \chi_\nu)}, \tag{8}$$

where c is the adiabatic sound speed.

The measurement points are set as x_1 and x_2, and the point just before the elastic membrane is set as x_3, as shown in Fig. 1. From Eq. (6)

$$U(x_1) = \frac{P(x_2) - m_{11}(x_1, x_2)P(x_1)}{m_{12}(x_1, x_2)} \tag{9}$$

is obtained. Equation (6) can be changed to be

$$\begin{pmatrix} P(x_3) \\ U(x_3) \end{pmatrix} = M(x_1, x_3) \begin{pmatrix} P(x_1) \\ U(x_1) \end{pmatrix} \tag{10}$$

and hence,

$$\begin{aligned} \begin{pmatrix} P(x_3) \\ U(x_3) \end{pmatrix} &= M(x_1, x_3) \begin{pmatrix} P(x_1) \\ \dfrac{P(x_2) - m_{11}(x_1, x_2)P(x_1)}{m_{12}(x_1, x_2)} \end{pmatrix} \\ &= M(x_1, x_3) \begin{pmatrix} 1 & 0 \\ \dfrac{-m_{11}(x_1, x_2)}{m_{12}(x_1, x_2)} & \dfrac{1}{m_{12}(x_1, x_2)} \end{pmatrix} \\ &\quad \times \begin{pmatrix} P(x_1) \\ P(x_2) \end{pmatrix} \end{aligned} \tag{11}$$

is obtained. Therefore, the simultaneous measurement of $P(x_1)$ and $P(x_2)$ yields $P(x_3)$ and $U(x_3)$.

Acoustic power, which is the time averaged rate of acoustic energy transmission through a cross section of the tube, is defined as

$$\begin{aligned} W(x) &= \frac{\omega S}{2\pi} \oint \mathrm{Re}[P(x)]\mathrm{Re}[U(x)]dt \\ &= \frac{S}{2} \mathrm{Re}\big[P(x)\tilde{U}(x)\big], \end{aligned} \tag{12}$$

where notation $\sim$ indicates the complex conjugate, and S is the cross-sectional area of the tube. The acoustic power at $x = x_3$, $W(x_3)$, is obtained using $P(x_3)$, $U(x_3)$, and Eq. (12). The amount of acoustic power dissipated in section 2, W_2, can be expressed as

$$W_2 = W(x_3) - \delta W_m, \tag{13}$$

where δW_m is the power dissipated by the membrane. This is because the acoustic power at the closed end ($x = x_4$) must be zero.

A. Preliminary experiment for evaluation of power dissipation due to membrane

To estimate δW_m, preliminary measurements are performed with and without the membrane while maintaining $|P(x_4)|$ at 90 Pa. The CH is dried and the room air is used as the working gas in both the sections in this preliminary experiment. The power dissipation δW_m can be estimated as

$$W(x_3) - W'(x_3) = \delta W_m, \tag{14}$$

where $W(x_3)$ and $W'(x_3)$ represent the power measured with and without the membrane, respectively. Note that the estimation of W through Eq. (6) requires the values of the gas properties. The properties of dry air are used because the "absolute" humidity of the room air is low ($<12\,\mathrm{g/m^3}$).

The measured values of $W(x_3)$, $W'(x_3)$, and δW_m are shown in Fig. 2 as a function of T_{gas}, which is varied in the next experiment. The measurements are performed using the

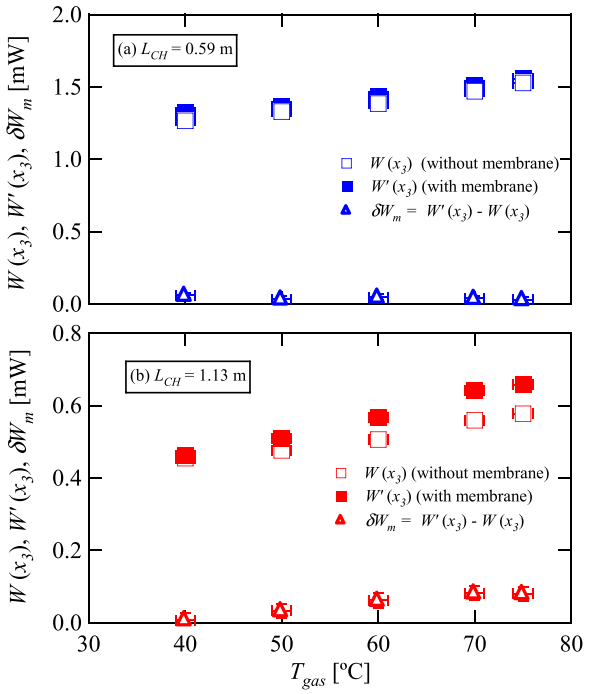

FIG. 2. (Color online) Result of the preliminary experiment. The acoustic power measured close to the center of the resonator with and without the membrane is shown as a function of T_{gas} by squares and the estimated dissipation due to the membrane is shown by triangles. The data were obtained (a) when the CH was located close to the velocity antinode ($L_{\mathrm{CH}} = 0.59$ m) and (b) when the CH was located close to the pressure antinode ($L_{\mathrm{CH}} = 1.13$ m).

two different honeycomb ceramic positions, i.e., $L_{CH} = 0.59$ m and $L_{CH} = 1.13$ m. The first position implies that the CH exists close to the velocity antinode, whereas the second position implies that it is close to the pressure antinode. As seen from Fig. 2, the dissipation in the membrane in considerably smaller than the dissipation in section 2. The ratio $\delta W_m/W'(x_3)$ is less than 0.15 and 0.05 when $L_{CH} = 1.13$ m and $L_{CH} = 0.59$ m, respectively. Moreover, it is found that δW_m changes as T_{gas} increases. This can be attributed to the fact that the increase in T_{gas} results in an increase in the wavelength of the input acoustic wave through an increase in sound speed. The increase in wavelength shifts the relative position of the membrane to the velocity (pressure) antinode and then the velocity amplitude at the membrane changes. As δW_m would depend on velocity amplitude, the measured δW_m depends on T_{gas}. These values of δW_m are considered in the analysis described in Sec. IV.

IV. EXPERIMENTAL RESULTS

The acoustic power dissipated in section 2, W_2^{wet}, is measured by inserting the CH containing 5 g water into section 2. As the maximum containable amount of water vapor in air increases with the temperature of air and anomalous sound propagation was observed close to the dew point,[18] T_{gas} is selected as a controlling parameter.

The experimental results for the case where the CH is located close to the velocity antinode ($L_{CH} = 0.59$ m) are shown in Fig. 3 by closed circles, where W_2^{wet} is normalized by the W_2 measured with the dried CH, W_2^{dry}. As seen from the figure, W_2^{wet}/W_2^{dry} does not depend on T_{gas} and its value is close to unity ($1.05 < W_2^{wet}/W_2^{dry} < 1.09$). This indicates that the water contained in the CH does not strongly affect the dissipation caused by velocity oscillation, namely, viscous dissipation. It should be noted that the formation of a water film on the wall of the CH cannot be visually observed, and hence, the flow channel radius in the CH would not be changed significantly by 5 g of added water.

Next, let us discuss the W_2^{wet}/W_2^{dry} measured under the condition that the wet CH is located close to the pressure antinode ($L_{CH} = 1.13$ m). As clearly shown in Fig. 3 by open circles, W_2^{wet}/W_2^{dry} increases with T_{gas} and reaches 1.7 at $T_{gas} = 75\,^{\circ}$C. This implies that the water contained on the wall of the CH contributes to acoustic dissipation even when T_{gas} is below the boiling point and that the impact of the water increases when T_{gas} increases to the boiling point.

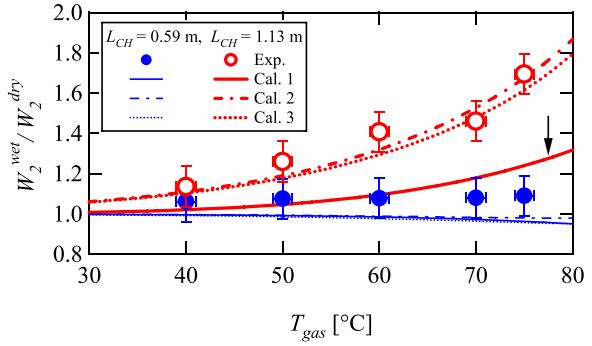

FIG. 3. (Color online) Dissipation ratio as a function of gas temperature. The dissipation in section 2 with dry CH is denoted as W_2^{dry}, whereas that with wet CH is denoted as W_2^{wet}. Symbols show the experimental results and lines show the calculation results.

The experimental results show that the water contained on the wall of the CH increases the dissipation caused by pressure oscillation, whereas the water has a small impact on the dissipation due to velocity oscillation. As pressure oscillation is accompanied by the oscillation of thermodynamic state properties such as temperature, it can cause the condensation and evaporation of water when there is a source of water. On the contrary, velocity oscillation does not directly yield the change in thermodynamic state properties. Therefore, the experimental results imply that evaporation and condensation play a key role in acoustic dissipation.

V. COMPARISON BETWEEN EXPERIMENTAL AND THEORETICAL RESULTS

Raspet *et al.* theoretically investigated the effect of evaporation and condensation on acoustic wave propagation.[5–7] They assumed a water film, whose thickness was zero, on a tube wall and considered mass transfer along the radial direction. We calculate W_2 using Raspet's and Rott's theories and compare them with the experimental results shown in Fig. 3. First, the equations used in Raspet's theory are mentioned and then the comparison is presented.

A. Raspet's theory

Raspet *et al.* extended Rott's theory to consider the effect of the water on the wall of the waveguide. Hence, the equations in Raspet's theory can be considerably similar to those in Rott's theory. The equations derived by Raspet *et al.* can be written as

$$\frac{dP}{dx} = -\frac{i\omega\rho_m}{1-\chi_v}U, \tag{15}$$

$$\frac{dU}{dx} = -[1+(\gamma-1)\chi_\alpha]\frac{i\omega P}{\gamma P_m} - \left[\frac{n_w}{n_a}\gamma\chi_D\right]\frac{i\omega P}{\gamma P_m}, \tag{16}$$

where n_w and n_a are the number density of water vapor and the number density of air, respectively; χ_D is the third thermoacoustic function.[5–7,19] As the cross section of the flow channels in the CH is square,[20] χ_α, χ_ν, and χ_D become

$$\chi_j = 1 - \frac{64}{\pi^4}\sum_{m,n\,\mathrm{odd}}\frac{1}{m^2n^2Y_j}, \tag{17}$$

with

$$Y_j = 1 - i\frac{\pi^2}{8\omega\tau_j}(m^2+n^2), \tag{18}$$

where j is α, ν, or D. To calculate τ_α and τ_ν in Eq. (5), half the length of one side of the square channel (0.47 mm) is used as r, and τ_D is defined as

$$\tau_D = r^2/(2D_{12}), \tag{19}$$

where D_{12} is the mutual diffusion coefficient, whose value can be obtained from the data book.[21]

Equation (15) is exactly equal to Eq. (1), whereas Eq. (16) differs from Eq. (2) by its second term on the right-hand side, which describes the effect of mass transfer. Equation (6) can be used as the solution of Eqs. (15) and (16). However, the following equation must be used instead of Eq. (7):

$$k_{\mathrm{wet}} = \frac{\omega}{c}\sqrt{\frac{1+(\gamma-1)\chi_\alpha}{1-\chi_\nu}+\frac{n_w}{n_a}\frac{\gamma\chi_D}{1-\chi_\nu}}. \tag{20}$$

To prevent misunderstanding, we define the wave number evaluated using Eq. (7) as k_{dry}. We should note that subscript dry indicates dry "wall" and not dry air.

The numerical calculation requires the values of gas properties and the ratio of n_w and n_a of humid air because the absolute humidity is high in section 2, as mentioned in Sec. II. In this study, the equations[22] based on the kinetic theory of gases and Dalton's law are used. Note that following the experimental condition, the sum of the partial pressures of air and water vapor is set to 101 kPa.

B. Comparison

We perform three types of calculation to verify the theory. Section 2 is divided into two parts for the calculation. One part is the interior of the CH and the other is the exterior. In all calculations, the gas properties of humid air, whose RH is 100%, are used for the interior of the CH. The RH outside the CH is set as 80% or 100%. This is because the RH measured outside the CH is over 80%. In the first calculation (Cal. 1), k_{dry} is used for the interior and exterior of the CH. In the second and third calculations (Cal. 2 and Cal. 3), k_{wet} is used for the interior and k_{dry} is used for the exterior. These conditions are shown in Table I.

The calculated results are shown in Fig. 3 by lines. As seen from Fig. 3, when the CH is located close to the pressure antinode ($L_{\mathrm{CH}} = 1.13$ m), the result of Cal. 1 (shown by the thick solid line indicated by an arrow in Fig. 3) is smaller than the experimental results shown by open circles. This indicates that the experimentally obtained increase in $W_2^{\mathrm{wet}}/W_2^{\mathrm{dry}}$ with T_{gas} cannot be explained by only the difference between the gas properties of dry air and humid air. On the contrary, the temperature dependence of $W_2^{\mathrm{wet}}/W_2^{\mathrm{dry}}$ for both cases ($L_{\mathrm{CH}} = 1.13$ m and 0.59 m) approximately agrees with the calculated results (Cal. 2 and Cal. 3), which are shown by dotted and dotted-and-dashed lines. Thus, this comparison supports the theory proposed by Raspet *et al.*

TABLE I. Calculation conditions. k_{dry} indicates the use of Eq. (7), whereas k_{wet} indicates the use of Eq. (20).

	In CH	Outside CH
Cal. 1	k_{dry}, RH = 100%	k_{dry}, RH = 100%
Cal. 2	k_{wet}, RH = 100%	k_{dry}, RH = 100%
Cal. 3	k_{wet}, RH = 100%	k_{dry}, RH = 80%

Rott's and Raspet's theories can explain the experimentally obtained dependency of $W_2^{\mathrm{wet}}/W_2^{\mathrm{dry}}$ on T_{gas} as follows: The dissipation of acoustic power can be written as

$$\Delta W = \int_{x_a}^{x_b}\frac{dW}{dx}dx = \int_{xa}^{x_b}\frac{d}{dx}\left(\frac{S}{2}\mathrm{Re}[P\tilde{U}]\right)dx. \tag{21}$$

When cross-sectional area S is constant,

$$\Delta W = \frac{S}{2}\int_{xa}^{x_b}\left(\mathrm{Re}\left[\frac{dP}{dx}\tilde{U}+\tilde{P}\frac{dU}{dx}\right]\right)dx. \tag{22}$$

Hence, Rott's theory [Eqs. (1) and (2)] shows

$$\Delta W = \frac{S}{2}\int_{xa}^{x_b}\left(R_{\mathrm{dry}}|U|^2+K_{\mathrm{dry}}|P|^2\right)dx, \tag{23}$$

where

$$R_{\mathrm{dry}} = \omega\rho_m\,\mathrm{Im}\left[\frac{1}{1-\chi_\nu}\right], \tag{24}$$

$$K_{\mathrm{dry}} = \frac{\gamma-1}{\gamma P_m}\omega\,\mathrm{Im}[\chi_\alpha]. \tag{25}$$

On the contrary, Raspet's theory [Eqs. (15) and (16)] gives

$$\Delta W = \frac{S}{2}\int_{xa}^{x_b}\left(R_{\mathrm{wet}}|U|^2+K_{\mathrm{wet}}|P|^2\right)dx, \tag{26}$$

where

$$R_{\mathrm{wet}} = \omega\rho_m\,\mathrm{Im}\left[\frac{1}{1-\chi_\nu}\right], \tag{27}$$

$$K_{\mathrm{wet}} = \frac{\gamma-1}{\gamma P_m}\omega\,\mathrm{Im}[\chi_\alpha]+\frac{n_w}{n_a}\,\mathrm{Im}[\chi_D]\frac{\omega}{P_m}. \tag{28}$$

The first terms on the right-hand side of Eqs. (23) and (26) are proportional to the square of velocity amplitude, whereas the second terms are proportional to the square of pressure amplitude. Furthermore, all of them have negative values, indicating a decrease in acoustic power. As $R_{\mathrm{wet}} = R_{\mathrm{dry}}$, which are relative to the first terms on the right-hand side of Eqs. (23) and (26), the theories indicate that the dissipation due to velocity oscillation does not depend on the water on the wall of the flow channel. This is consistent with the experimental results. On the contrary, K_{wet} has an additional term, which is the second term of the right-hand side of Eq. (28). As this term has a negative value, the theories indicate that the water on the wall affects the dissipation caused by pressure oscillation. In addition, the second term is proportional to n_w/n_a. The coefficient n_w/n_a increases as the temperature of water approaches its boiling point if RH is maintained at a constant value. Hence, the effect of the second term increases with T_{gas}, resulting in the increase in $W_2^{\mathrm{wet}}/W_2^{\mathrm{dry}}$. These results indicated by the theories are also consistent with the experimental results.

VI. CONCLUSION

The acoustic dissipation in a wet-wall porous medium was measured. The experimental results indicated that the dissipation caused by acoustic velocity oscillation was not affected by the water on the wall of the porous medium. On the contrary, the dissipation caused by acoustic pressure oscillation was affected by water, particularly when the temperature of the working gas was close to the boiling temperature of water. These results were compared with the results calculated based on the theory proposed by Raspet *et al.*,[5–7] and the validity of the theory was demonstrated.

ACKNOWLEDGMENTS

This work was supported by JSPS KAKENHI Grant No. 17K17705.

[1]H. Tijdeman, "On the propagation of sound waves in cylindrical tubes," J. Sound Vib. **39**, 1–33 (1975).
[2]T. Yazaki, Y. Tashiro, and T. Biwa, "Measurements of sound propagation in narrow tubes," Proc. Royal Soc. London, Ser. A **463**, 2855–2862 (2007).
[3]B. I. Pandit and M. S. King, "The variation of elastic wave velocities and quality factor q of a sandstone with moisture content," Can. J. Earth Sci. **16**, 2187–2195 (1979).
[4]Y. Mao, "Sound attenuation in a cylindrical tube due to evaporation-condensation," J. Acoust. Soc. Am. **104**, 664–670 (1998).
[5]R. Raspet, C. Hickey, and J. Sabatier, "The effect of evaporation-condensation on sound propagation in cylindrical tubes using the low reduced frequency approximation," J. Acoust. Soc. Am. **105**, 65–73 (1999).
[6]C. Hickey, R. Raspet, and W. Slaton, "Effects of thermal diffusion on sound attenuation in evaporating and condensing gas-vapor mixtures in tubes," J. Acoust. Soc. Am. **107**, 1126–1130 (2000).
[7]R. Raspet, W. Slaton, C. Hickey, and R. Hiller, "Theory of inert gas-condensing vapor thermoacoustics: Propagation equation," J. Acoust. Soc. Am. **112**, 1414–1422 (2002).
[8]C. Guianvarc'h, M. Bruneau, and R. M. Gavioso, "Acoustics and precondensation phenomena in gas-vapor saturated mixtures," Phys. Rev. E **89**, 023208 (2014).
[9]D. Noda and Y. Ueda, "A thermoacoustic oscillator powered by vaporized water and ethanol," Am. J. Phys. **81**, 124–126 (2013).
[10]K. Tsuda and Y. Ueda, "Abrupt reduction of the critical temperature difference of a thermoacoustic engine by adding water," AIP Adv. **5**, 097173 (2015).
[11]K. Tsuda and Y. Ueda, "Critical temperature of traveling- and standing-wave thermoacoustic engines using a wet regenerator," Appl. Energy **196**, 62–67 (2017).
[12]T. Biwa, Y. Tashiro, U. Mizutani, M. Kozuka, and T. Yazaki, "Experimental demonstration of thermoacoustic energy conversion in a resonator," Phys. Rev. E **69**, 066304 (2004).
[13]T. Biwa, Y. Ueda, T. Yazaki, and U. Mizutani, "Work flow measurements in a thermoacoustic engine," Cryogenics **41**, 305–310 (2001).
[14]N. Rott, "Damped and thermally driven acoustic oscillations," Z. Angew. Math. Phys. **20**, 230–243 (1969).
[15]G. W. Swift, *Thermoacoustics: A Unifying Perspective for Some Engines and Refrigerators* (Acoustical Society of America, PA, 2002).
[16]A. Tominaga, *Fundamental Thermoacoustics* (Uchidarokakumo, Tokyo, 1998).
[17]Y. Ueda and C. Kato, "Stability analysis for spontaneous gas oscillations thermally induced in straight and looped tubes," J. Acoust. Soc. Am. **124**, 851–858 (2008).
[18]J. B. Mehl and M. R. Moldover, "Precondensation phenomena in acoustic measurements," J. Chem. Phys. **77**, 455–465 (1982).
[19]W. V. Slaton, R. Raspet, C. J. Hickey, and R. A. Hiller, "Theory of inert gas-condensing vapor thermoacoustics: Transport equations," J. Acoust. Soc. Am. **112**, 1423–1430 (2002).
[20]W. Arnott, H. Bass, and R. Raspet, "General formulation of thermoacoustics for stacks having arbitrarily shaped pore cross sections," J. Acoust. Soc. Am. **90**, 3228–3237 (1991).
[21]*JASM Data Book: Thermophysical Properties of Fluids* (Japan Society of Mechanical Engineers, Tokyo, 1983).
[22]S. Ooe, *Bussei Teisuu Suisan Hou (Physical Property Estimation Methods)* (Nikkann Kougyou Shinbunsha, Tokyo, 1985).